FREE-ELECTRON LASER RESULTS FROM THE ADVANCED TEST ACCELERATOR

T. J. Orzechowski, J. L. Miller, J. T. Weir, Y. -P. Chong,
F. Chambers, G. A. Deis, A. C. Paul, D. Prosnitz, and E. T. Scharlemann
Lawrence Livermore National Laboratory*
Livermore, California

K. Halbach
Lawrence Berkeley Laboratory†
Berkeley, California

J. Edighoffer
TRW, Inc.
Redondo Beach, California

ABSTRACT

PALADIN is a 10.6-μm FEL amplifier experiment operating at the Lawrence Livermore National Laboratory's Advanced Test Accelerator, an induction linear accelerator designed to produce a 45-MeV, 10-kA electron beam. With a 15-m long wiggler, PALADIN demonstrated 27 dB of exponential gain from a 14-kW input signal. With a 5-MW input signal, the amplifier saturated after 10 dB of gain. The exponentially growing signal in the unsaturated amplifier was clearly seen to be gain guided by the electron beam.

INTRODUCTION

The high gain, high output power, and high extraction efficiency expected from a tapered-wiggler FEL amplifier were demonstrated in 1986 on ELF[1] (Electron Laser Facility), a microwave FEL using an 850-A, 3.5-MeV electron beam from LLNL's Experimental Test Accelerator (ETA). ELF achieved an output power of 1 GW with 35% extraction efficiency (i.e., conversion of electron beam power to microwave power). The ELF experiment, while demonstrating the basic physics of a high-gain, tapered-wiggler FEL amplifier, was operated in a waveguide and so left unresolved some issues, such as gain guiding, refractive guiding, and optical mode cleanup, associated with signal propagation in an optical FEL.

The PALADIN experiment has been designed to address the optical FEL physics issues that could not be addressed in ELF. In addition, the PALADIN experiment uses a novel electron beam focusing technique[2]: specially shaped magnet pole faces provide a sextupole-like field that focuses the beam equally in both horizontal and vertical directions.

EXPERIMENT

PALADIN operates as an FEL amplifier at 10.6 μm (CO_2 laser wavelength). It uses the electron beam produced by the Advanced Test Accelerator (ATA)[3] at the Lawrence Livermore National Laboratory. The electron beam has an energy of 45 MeV. The electron beam is scraped by an emittance filter, after which the electron beam is transported through an achromatic jog onto a parallel beamline that includes the wiggler magnet. The input signal (provided by a CO_2 laser) is injected at the final bend in the achromatic jog and copropagates with the electron beam through the wiggler. At the end of the wiggler the electron beam is deflected into a beam dump, while the optical pulse is relayed to a diagnostic station where its total power and mode profile are measured. The PALADIN experiment is illustrated in Fig. 1.

The Advanced Test Accelerator is a linear induction accelerator (LIA) with a 2.5 MeV injector and 190 accelerator cells, each capable of giving the electron beam an energy increment of 0.25 MeV. While ATA is designed to produce 10-kA beams, we typically accelerate 2.5 to 3 kA for the FEL experiment. Beam loading drops the overall energy to 45 MeV. The electron beam is focused through the accelerator by an ion channel created by photoionization of a low pressure (~0.1 mT) benzene (C_6H_6) channel.[4] At the end of the accelerator, the ion focus is terminated, and the electron beam is focused with magnetic quadrupoles.

A variable acceptance emittance filter is used to scrape electrons with unacceptably high emittance while reducing the overall electron current. The emittance filter is composed of an array of five quadrupole doublets and six range thin foils with apertures in them.
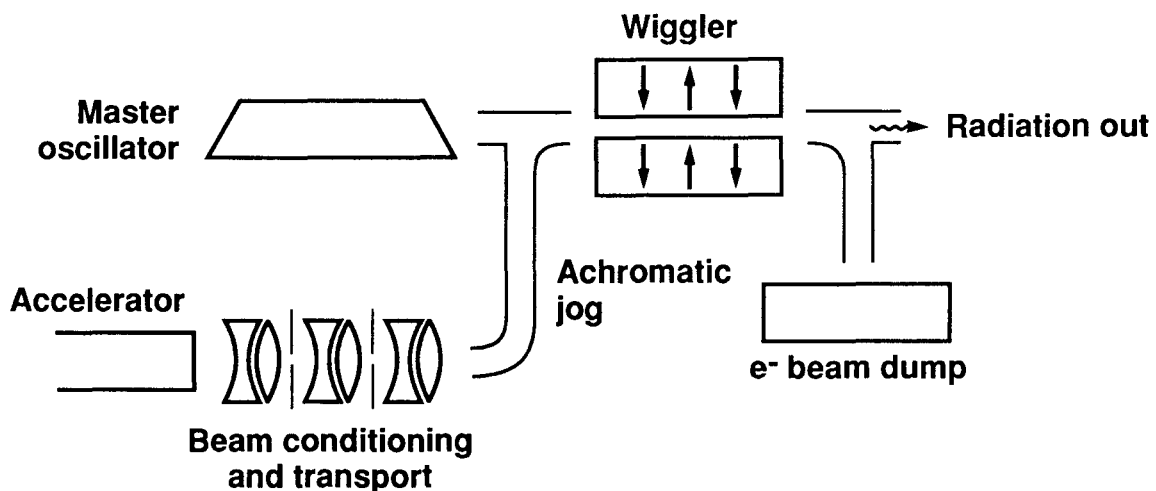

Figure 1. Schematic of an optical free-electron laser amplifier.

This device is shown schematically in Fig. 2. The beam size at the foils is a function of emittance. High emittance electrons strike the foil (rather than pass through the aperture) and are scattered to the vacuum pipe wall. The phase space of the emerging electron beam is a dodecagon (12 sided polygon). The acceptance of such an emittance filter, for the geometry used in this experiment, is determined numerically for different quadrupole excitations.

The achromatic jog is composed of four dipole magnets: two 45° bend magnets and two 79° bend magnets. The achromatic jog is designed to accept a ±2% energy sweep with an emittance range of 1-3 π cm-mrad. Within this range both the phase space orientation and the beam trajectory will be preserved (i.e., angle out is the same as angle in). At the last magnet of the achromatic jog the input signal from a CO_2 laser is injected along the beam axis so that both the input signal and electron beam are on the same axis through the wiggler.

After the beam emerges from the achromatic jog, two quadrupole doublets are used to match the electron beam into the wiggler magnet. Return current monitors and viewing foils in the wiggler matching section are used to measure the beam position and transverse profile to ensure a good match into the wiggler.

The wiggler magnet is an iron core, dc electromagnet with permanent magnet assist to allow for a larger tuning range before the iron core saturates.[5,6] The wiggler period is 8 cm, and the wiggler is constructed in 5-m-long modules. The wiggler gap is 3 cm at the widest part, permitting a design field of 2.5 kG with less than 1% magnetic losses in the iron. The ultimate design length of the PALADIN wiggler is 25 m, although for the experiments discussed below, a 15-m wiggler was used. A schematic of one wiggler period is shown in Fig. 3. The poles are specially shaped to provide horizontal focusing[2] (in the wiggle plane), while the wiggler field itself provides vertical focusing. The wiggler field with the shaped pole pieces is approximately given by

$$\mathbf{B}_\mathrm{w} = B_\mathrm{o} \left[\cosh k_x x \cosh k_y y \cos k_\mathrm{w} z \, \hat{y} \right.$$
$$+ \left(\frac{k_x}{k_y} \right) \sinh k_x x \sinh k_y y \cos k_\mathrm{w} z \, \hat{x}$$
$$\left. + \left(\frac{k_\mathrm{w}}{k_y} \right) \cosh k_x x \sinh k_y y \sin k_\mathrm{w} z \hat{z} \right] \, , \qquad (1)$$

with

$$k_x^2 + k_y^2 = k_\mathrm{w}^2 \, .$$

This form of wiggler field gives equal focusing in both the x and y dimensions when $k_x = k_y = k_\mathrm{w}/\sqrt{2}$, resulting in a round electron beam through the wiggler. More important, this field ensures that the longitudinal velocity, β_parallel ($\equiv v_{\parallel}/c$) of an electron, when averaged over a wiggle period, remains constant over a betatron period. Without this important property, the electrons could detrap from the ponderomotive well with serious consequences for FEL performance.[2]
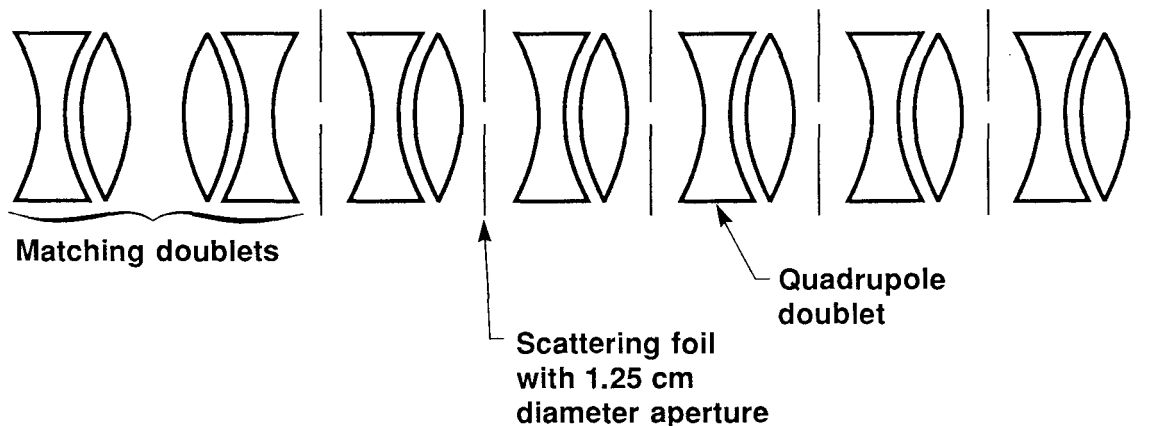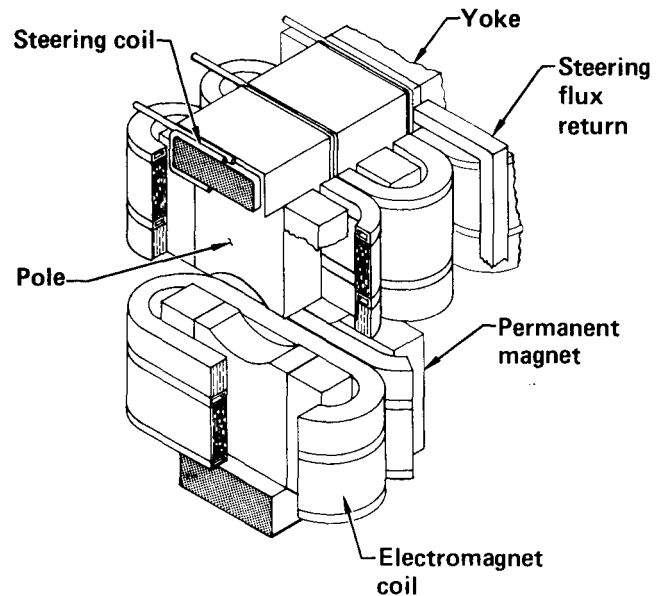

Figure 3. Schematic of one period of PALADIN wiggler.

Each two periods of the wiggler is connected to its own power supply to provide for flexibility in tuning the wiggler field profile (e.g., tapering). Care must be taken when energizing an iron core wiggler so as not to introduce any steering. For this reason, a steering free excitation pattern is used to energize the wiggler. This pattern is a 1-2-1 winding pattern.[7]

The vacuum pipe through the wiggler is a 2.54-cm-diam tube. The tube has symmetric access ports approximately every 1.5 m down the length of the device. This allows for vacuum pumping and electron beam diagnostics.

Line-of-sight targets, called pop-in probes, can be inserted into the wiggler, and the beam profile is monitored with gated cameras. The betatron wavelength is given by

$$k_{\beta_{x,y}} = \frac{eB_\mathrm{w}}{2\gamma mc} \, . \qquad (2)$$

For the PALADIN experiment the betatron wavelength is about 10 m; thus, there are six probes per betatron wavelength, and the beam trajectory can be monitored through the wiggler.

The input signal is provided by a CO_2 laser operating at 10.6 μm. The system consists of an oscillator and an amplifier. The oscillator produces a single longitudinal mode and has a 50-ns pulse length. The input power is either 14 kW (oscillator only) or

Matching doublets

Scattering foil with 1.25 cm diameter aperture

Quadrupole doublet

Figure 2. Schematic of the quadrupole emittance selector.

5 MW (oscillator and amplifier). An input telescope focuses the optical beam to a waist at the entrance to the wiggler with a $1/e^2$ radius of 4 mm (Rayleigh range = 4.7 m).

The output diagnostics consist of HgCdTe detectors: one measuring total power in the image plane located at the end of the wiggler and another measuring the central peak intensity of the image. A calorimeter monitors total laser beam energy and a pyroelectric vidicon measures the intensity distribution of the optical signal at the end of the wiggler.

RESULTS

In measuring the beam brightness using the quadrupole emittance selector, we find that the electron beam does not have a uniform brightness. That is, the current transmitted through the quadrupole emittance selector (QES) does not scale with the square of the acceptance, as would be expected if the electron beam's phase space was uniformly filled and larger than the acceptance of the QES. This nonuniform phase space distribution is illustrated in Fig. 4, where we have plotted brightness (proportional to $I_{transmitted} \div$ acceptance^2) as a function of transmitted current. If phase space were uniformly filled, the brightness would remain constant. The 3-kA beam is composed of a relatively bright 300-A core ($J_{core} \cong 1.3 \times 10^8$ A/(rad-m)^2) and a lower quality (i.e., lower brightness) beam (2700 A) with a Gaussian emittance profile with $\varepsilon_{1/e} = 2.67 \times 10^{-3}$ m-rad (normalized). Typically, we take 500–700 A through the emittance selector and wiggler. Thus, the beam used in PALADIN is composed of two components: the bright core and the less bright Gaussian emittance profile beam with $\varepsilon_{n,max} = 2.36 \times 10^{-3}$ m-rad.

With this electron beam, we measure the FEL gain and detuning profiles with a 15-m-long wiggler and 14-kW input. The result of the detuning measurement (P_{out} vs B_w) is shown in Fig. 5. The peak
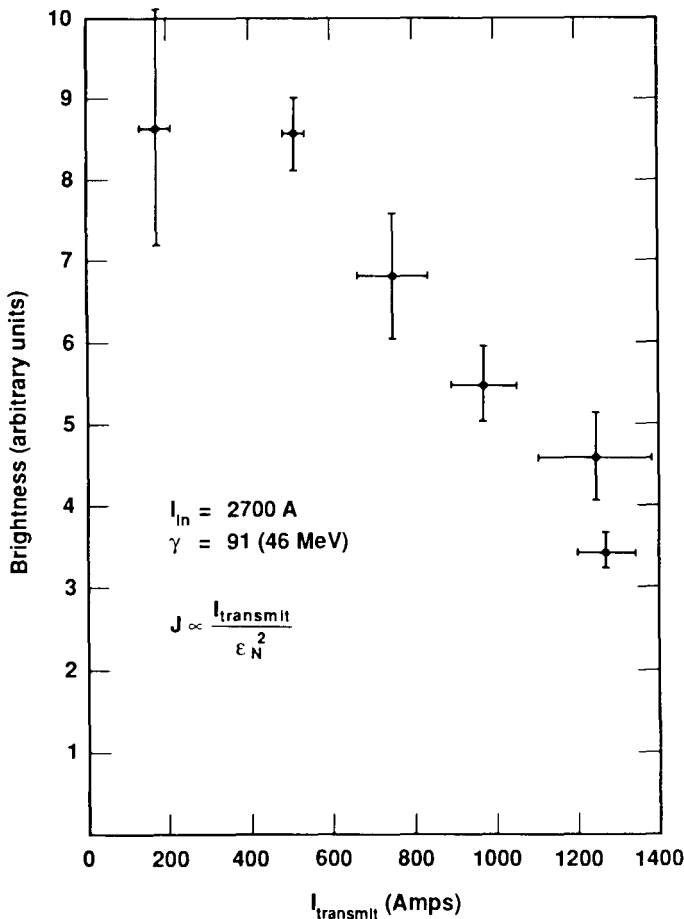
of the detuning curve occurs at 1960 G. This is in good agreement with the expected wiggler field for an FEL operating at 10.6 μm and using a 45-MeV electron beam. Using this value for the resonant wiggler field, we varied the length of the wiggler by turning the nonresonant part of the wiggler to a value of $0.7 \times B_{w,res}$. This nonresonant part of the wiggler field, while not contributing to the FEL performance, focuses the electron beam through the wiggler, after which it is bent by a dipole magnet to an electron beam dump. The result of this gain measurement is shown in Fig. 6. The overall power gain for this configuration is 27 dB (×500). The gain does not appear to be uniform over the 15-m wiggler but appears to have regions of higher and lower gain. This is not completely understood, but numerical simulations with the computer code FRED do show some structure in the gain profile.

In Figs. 5 and 6, two curves are plotted for each measurement: a total power curve and a peak intensity curve. It is seen that the peak intensity grows faster than the total power. The discrepancy between the two curves is explained by gain guiding. The waist of the optical signal (originally located at the entrance to the wiggler by the focus of the input signal) is shifted by the high gain medium, to the end of the amplifier region. Thus, at the end of the wiggler, where the radiation signal is measured (image plane for output diagnostics), not only has the total power increased, but the radiation profile is narrower. This phenomenon is recorded in Fig. 7. With no gain, the input signal diffracts while passing through the wiggler ($L_{wiggler} > 3\,z_R$, where $z_R \equiv$ Rayleigh range). By the end of the wiggler, the input signal fills the 2.54-cm-diam tube, and one can observe a diffraction ring forming in the image of the output signal at the output of the wiggler. In the high gain case, the output signal at the end of the wiggler is a small spot (~1 cm diam) which corresponds to the size of the electron beam. The diffraction losses are masked by the high gain of the FEL amplifier and the radiation signal takes on the shape of the gain medium (electron beam).

With the 14-kW signal and 27 dB of gain, the FEL output reaches 7 MW. The FEL shows no sign of saturating. Increasing
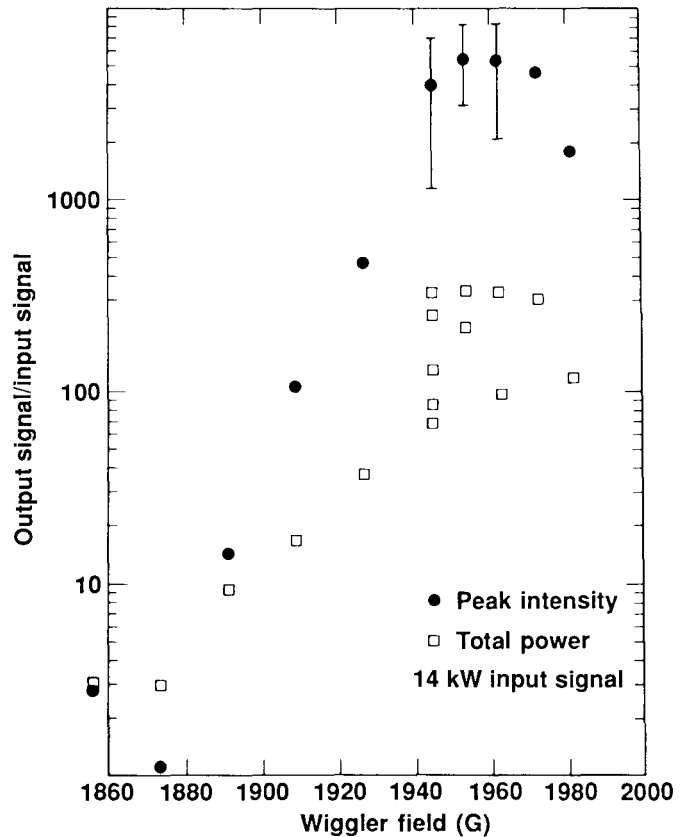

Figure 4. Beam brightness (arbitrary units) as function of current transmitted through quadrupole emittance selector.

Figure 5. Gain (power out/power in) as a function of wiggler field for the 15-m long wiggler and input power of 14 kW (I_{beam} = 500 A).

the input signal to 5 MW we again measure the gain of the amplifier at the peak of the detuning curve. The results of measurement are shown in Fig. 8. The amplifier appears to saturate midway through the wiggler with the power gain substantially reduced in the latter part of the wiggler.

Future PALADIN experiments will concentrate on improving the quality of the electron beam as well as increasing the wiggler length to 25 m. Investigations are currently under way to find the cause of the two-component distribution.

REFERENCES

1. T. J. Orzechowski, B. R. Anderson, J. C. Clark, W. M. Fawley, A. C. Paul, D. Prosnitz, E. T. Scharlemann, S. M. Yarema, D. B. Hopkins, A. M. Sessler, and J. S. Wurtele, "High-Efficiency Extraction of Microwave Radiation from a Tapered-Wiggler Free-Electron Laser," Phys. Rev. Lett. **57**, 2172 (1986).
2. E. T. Scharlemann, "Wiggle Plane Focusing in Linear Wigglers," J. Appl. Phys. **58**, 2154 (1985).
3. L. L. Reginato, "The Advanced Test Accelerator (ATA), a 50 MeV, 10 kA, Induction Linac," IEEE Trans. Nucl. Sci. **NS-30**, 2970 (1983).
4. W. E. Martin, G. J. Caporaso, W. M. Fawley, D. Prosnitz, and A. G. Cole, "Electron-Beam Guiding and Phase-Mix Damping by a Laser-Ionized Channel," Phys. Rev. Lett. **54**, 685 (1985).
5. K. Halbach, "Some Concepts to Improve the Performance of DC Electromagnetic Wigglers," Nuc. Instrum. Meth. **A250**, 115 (1986).
6. G. A. Deis, A. R. Harvey, C. D. Parkison, D. Prosnitz, J. Rego, E. T. Scharlemann, and K. Halbach, "A Long Electromagnetic Wiggler for the PALADIN Free-Electron Laser Experiment," IEEE Trans. Magnetics **24**, 1090 (1988).
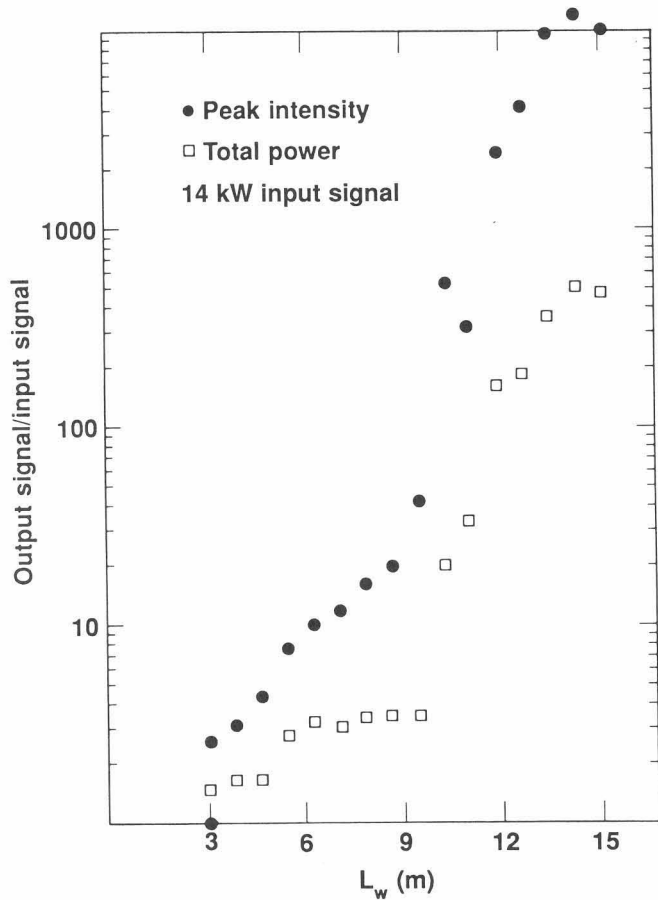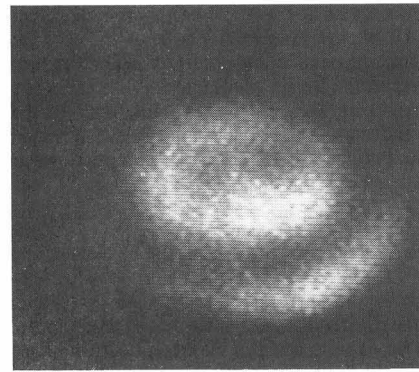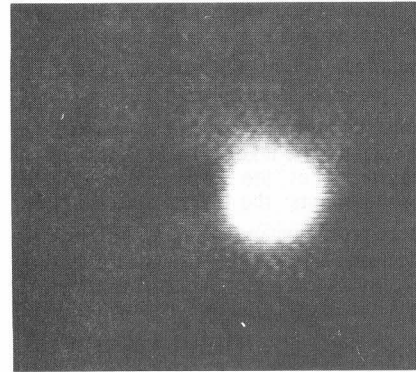7. K. Halbach, "Desirable Excitation Patterns for Tapered Wigglers," Nuc. Instrum. Meth. **A250**, 95 (1986).

Master oscillator only
(focus at wiggler entrance)

Master oscillator + FEL gain

Figure 7. Optical image at end of wiggler without (left) and with (right) high gain demonstrating gain guiding.

Figure 6. Gain (power out/power in) as function of wiggler length for $B_w = 1960$ G and input power of 14 kW ($I_{beam} = 500$ A).
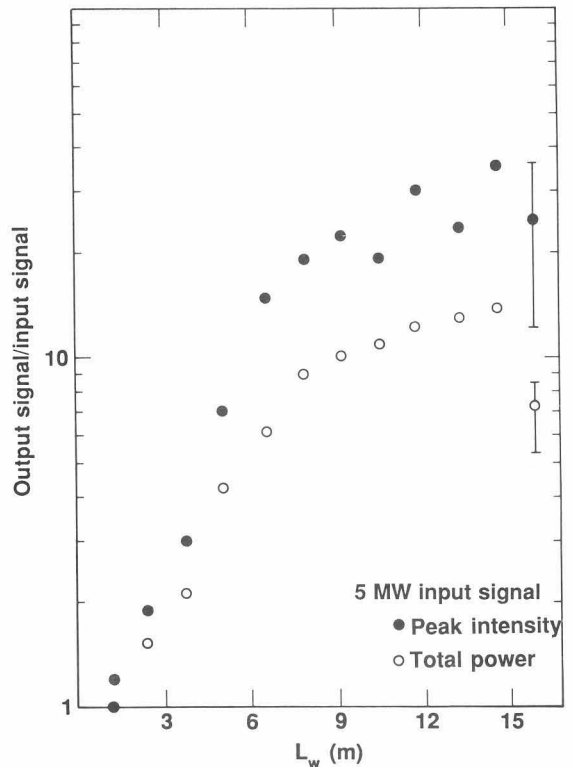

Figure 8. Gain (power out/power in) as a function of wiggler length for $B_w = 1960$ G and input power of 5 MW ($I_{beam} = 500$ A).